

Parameter Optimization and Development of Prediction Model for Second Generation Magnetic Abrasive Polishing of AZ31B Plate

Jae-Seob Kwak, Chang-Min Shin

Abstract—A conventional magnetic abrasive polishing (MAP) is not suitable for non-magnetic materials. The system with a electro-magnet array table installed under the working area of the non-magnetic material, which is called second generation MAP in this study, can help to enhance the magnetic force. Experimental evaluation and optimization of process parameters for MAP of AZ31B plate that is one of the non-magnetic materials were performed by a design of experiments and the response surface method. As a result, it is indicated that magnetic force intensity of magnetic table and spindle speed of inductor were significant parameters on improvement of surface roughness in the second generation MAP process. Therefore, prediction model of surface roughness was developed using second-order response surface method and signal to noise ratio.

Index Terms—Second generation MAP, Electro-magnet array table, Response surface model

I. INTRODUCTION

MAGNESIUM alloys are the lightest currently used as structural metals and honored as the 21st century green structural material. Owing to many advantages such as excellent mechanical properties, good machinability, good electromagnetic shielding characteristic and high dimensional stability, magnesium alloys have great application potential in aerospace, automobile and electronic device fields [1-4]. With the development of these industries, more precise surface of magnesium materials is naturally needed to meet the high quality of products. However, there are some limitations in producing good surface for magnesium materials due to fundamental problems such as flammability hazard and fragility properties. [5]

Magnetic abrasive polishing (MAP) was proposed as one of non-traditional techniques to overcome these difficulties. [6] In the MAP process, a polishing tool that consists of ferrous particles and non-ferrous abrasives under silicone oil medium has flexibility. This flexible tool can remove a very small amount of materials from a workpiece and then a better surface can be produced without damages on the surface.[7] Nevertheless, it is very difficult to adopt MAP for polishing of non-magnetic materials because magnetic force on the

working field determine the efficiency of this process. Therefore, it is necessary to improve magnetic force on artificially the surface of non-magnetic material during MAP process. Kwak[8] showed that improving strategy of magnetic force using permanent magnet, which installed in the opposite side of non-magnetic material, was very effective for enhancing the surface roughness and the rotational speed of the magnetic tool had a dominant effect on the improvement of surface roughness in the case of polishing of thin magnesium plate with the permanent magnet. Wang [9] has developed a novel magnetic abrasive medium to resolve the efficiency and recycling problem of the magnetic abrasive finishing (MAF) of an inner pipe using the silicone gel to mix steel grit and silicone carbon. As a result of study, the silicone gel medium had a good effect on the surface roughness and the material removal rate, especially in the non-magnetic field. Therefore, silicone gel medium is very useful to MAP of non-magnetic materials since it could constrain iron powder and abrasives efficiently.

In this study, the second generation magnetic abrasive polishing process, which consists of electro-magnet array table and magnetic abrasives mixed with silicone gel medium, was developed to improve the magnetic force for MAP of AZ31B magnesium alloy. The large number of process parameters affect on the surface roughness of non-magnetic materials after second generation MAP more than the conventional MAP process. Therefore, evaluation and optimization of process parameters such as current of magnetic array table was performed on basis of design of experiment. Moreover, the prediction models using response surface method and signal to noise ratio were developed to predict the enhanced surface roughness in the second generation MAP of AZ31B magnesium alloy.

II. SECOND GENERATION MAGNETIC ABRASIVE POLISHING

A. Characteristic of Second Generation Magnetic Abrasive Polishing

Fig. 1 represents the polishing mechanism of magnetic abrasive polishing for non-magnetic materials. A case where permanent magnet was not installed under the workpiece, the moment force of abrasive particle is easily increased since magnetic abrasives which consist of ferrous particles and non-ferrous particles were difficult to transmit the magnetic force to the surface of workpiece. As a result of this situation, cutting capability of magnetic abrasive polishing is reduced.

J. S. Kwak Department of Mechanical Engineering Pukyong National University Nam-Gu, Busan, South Korea (phone: +82-51-629-6139; e-mail: jskwak5@pknu.ac.kr).

C. M. Shin Department of Mechanical Engineering Pukyong National University Nam-Gu, Busan, South Korea (e-mail: scmfor@nate.com).

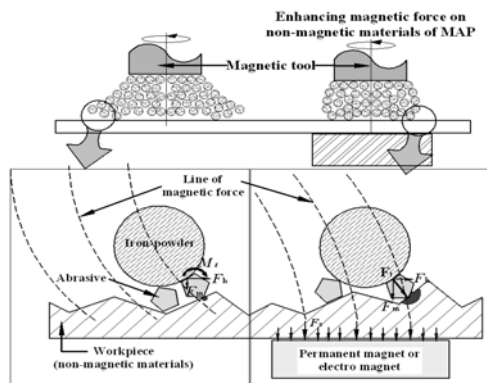


Fig. 1 Schematic of mechanism on MAP of non-magnetic material.

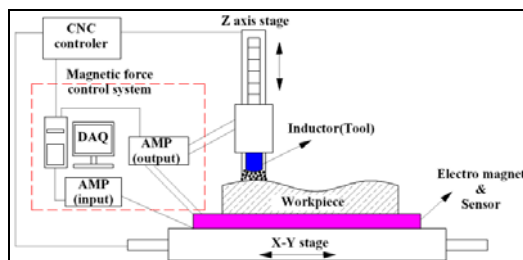


Fig. 2 Schematic of second generation magnetic abrasive polishing process.

On the other hand, as case where permanent magnet was installed under the non-magnetic material, magnetic abrasives could easily remove the material because of improved magnetic force by a permanent magnet.

The second generation magnetic abrasive polishing contains CNC controller and electro-magnet array table, which can improve the magnetic force on the surface of workpiece efficiently and control the magnetic flux density by changing of current value as shown in Fig. 2.

B. Electro-magnet Array Table

The electro-magnet array table was installed on the bad of MAP apparatus on a level with the magnetic tool as shown in Fig. 3. The electro-magnet array table used in this study includes 32 electro-magnets. Each electro-magnet was arranged at regular interval and could change the magnetic flux density by changing of a mount of current applied into coil. Moreover, that could reverse the magnet pole by using array table controller.

Each solenoid was formed by winding copper wire of $\varnothing 0.8$ diameter and 4750 turns around the core. The maximum value of magnet flux density generated on each core was about 20mT as 0.8A of current was supplied into coil. To improve the magnetic flux density generated on the surface of electro-magnet array table, non-magnetic materials were chosen as material of core and table bad.

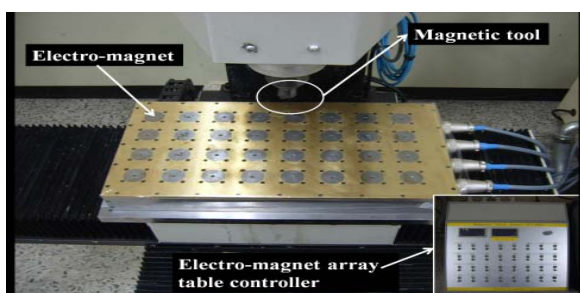


Fig. 3 Installed electro-magnet array table and controller.

III. INCREASING MAGNETIC FLUX DENSITY BY ELECTRO-MAGNET ARRAY TABLE

A. Simulation and Experimental Verification of Magnetic Flux Density for Single Row Electro-magnet

To evaluate magnetic characteristic of non-magnetic material in case of the second generation MAP process, a computer simulation was conducted. The magnetic characteristics concerned in this simulation were the distribution and the maximum magnitude of the magnetic flux density on the work material in accordance with change of array and magnet pole of electro-magnets. Magnetic flux density according to arrangement of magnet pole in 1 by 3 array of electro-magnets was simulated using a commercial software ANSYS. Fig. 4 (a) and (b) show the magnetic flux density on the work material with 1 by 3 array of electro-magnets. As magnet pole of 3 electro-magnets was same to N pole, the maximum magnitude, which was calculated at 19.201mT, was founded on the edge of work material. On the other hand, as magnet pole located at center of array was set to S pole, the maximum magnitude was presented in the center of work material and calculated at 42.552mT. These results revealed that intersection of magnet pole had good effect on improving magnetic flux density.

Fig. 5 shows the experimental setup and measuring points of the magnetic flux density. A thin probe of a Tesla meter(TM-601, KANETEC) was used for gaining the measuring values. The thickness of the probe was 1mm. Fig. 6 (a) and (b) show comparison of simulated magnitude with measured magnetic flux density. As results of experimental verification in case of that identical magnet pole was arranged, measured magnitudes were some different from simulated magnitudes. However, distribution of magnetic flux density was very similar to simulation results. On the other hand, in case that different magnet pole lined up alternately, both of distribution and maximum magnitude of measured magnetic flux density coincide well with those of the computer simulation. In these figures, minus sign means S pole of electro magnet.

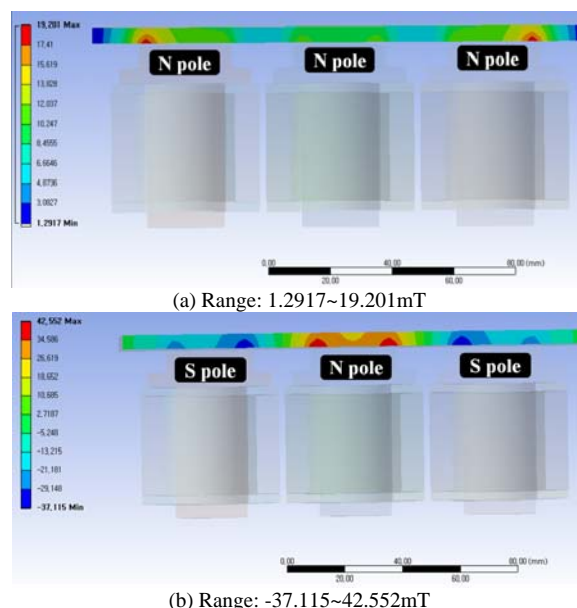


Fig. 4 Simulation results for magnetic flux density on a workpiece according to the array of electro- magnets.

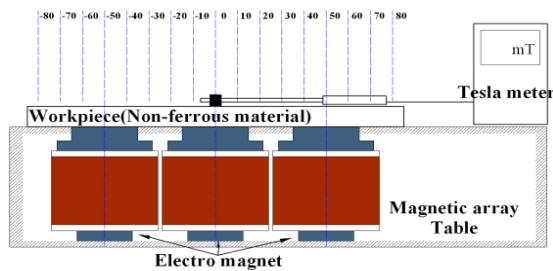


Fig. 5 Measuring method and points for magnetic flux density.

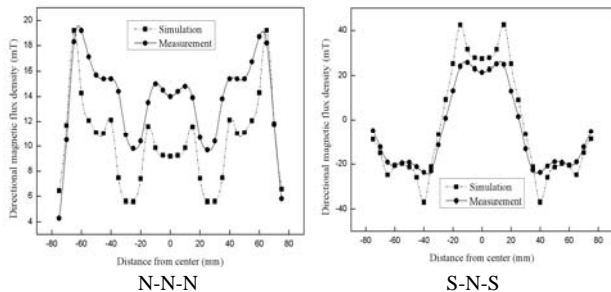


Fig. 6 Experimental verification for magnetic flux density.

B. Characteristic of Magnetic Flux Density for Multi Array Electro-magnets

The electro-magnet table used in this study was formed with multi array electro-magnets. Therefore, the same improving strategy of magnetic force with single array electro-magnets was applied. To verify the characteristic of that improving strategy, a series of experimental verification was performed. Fig. 7 indicated measuring method of magnetic flux density for 3 by 3 array electro-magnet. Fig. 8 (a) and (b) show result of experiments. As the working area which is set to N pole was surrounded with same magnet pole with N pole, the maximum magnitude of magnetic flux density was about 25mT. However, surrounded with S pole, the maximum magnitude was about 45mT. These results indicated that proposed method had good effect on improvement of magnetic force for electro-magnet table. Therefore, this proposed method was used in second generation MAP of magnesium alloy.

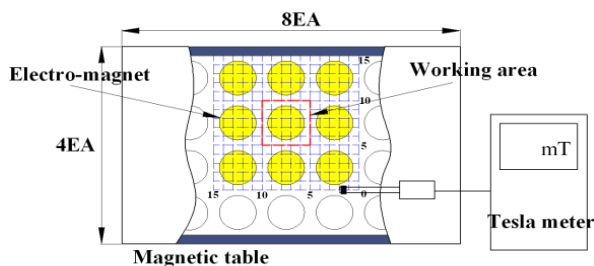


Fig. 7 Coordinates of measuring points for the magnetic flux density.

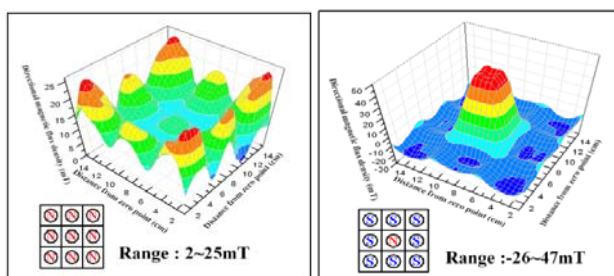


Fig. 8 Magnetic flux density of working area on electro-magnet array table.

IV. EVALUATION AND OPTIMIZATION OF MAP PARAMETERS

A. Experimental Procedure and Setup

For evaluating that which parameter is most effect on enhanced surface roughness, and finding optimal process condition for second generation of AZ31B, Taguchi’s design method was performed in this study. Fixed experimental conditions for evaluation of MAP parameters were indicated as shown in Table I . The work material used was AZ31B magnesium alloy which is length of 80mm, height of 60mm and thickness of 2mm. Magnetic abrasives mixed with ferromagnetic particles and abrasives in silicone gel were used in this experiment as a tool for polishing. The ferromagnetic particle was iron powder of 150µm, and the green carbide (GC) of mesh of 3000 was chosen as abrasives. The silicone gel could efficiently constrain iron powder and GC grain on the surface of non-magnetic material because of high viscosity of silicone gel medium. Given that the short working gap can identify the large magnetic force in MAP process, the working gap between the magnetic tool and work material was set to 1.5mm. The diameter of inductor tool was 20mm. Fig. 9 illustrates the experimental setup and procedure. As shown in Fig. 9, magnetic inductor tool passed periodically on the surface of workpiece during 5 minutes.

In this study, a current of table, a current of tool, a spindle speed and weight of magnetic abrasive were considered as experimental factors which would influence the surface roughness on the second generation MAP of AZ31B. All selected experimental factors were changed at three levels as listed in Table II. The factor of the current of table means amount of a current supplied into electro-magnet arranged in electro-magnet array table. The magnetic flux density was about 45mT when the supplied current was 0.8A. On the other hand, when a current of tool which means amount of a current supplied into the inductor was 2.5A, the maximum magnitude

TABLE I
FIXED CONDITIONS FOR EXPERIMENTS

Items	Conditions
Workpiece	AZ31B(80 x 60 x 2)
Magnetic abrasive	GC grain(8.5 µm)+Iron powder(150 µm) +Silicone gel(300,000cs)
Working gap	1.5mm
Working time	5min
Feed rate	4m/min
Tool diameter	20mm

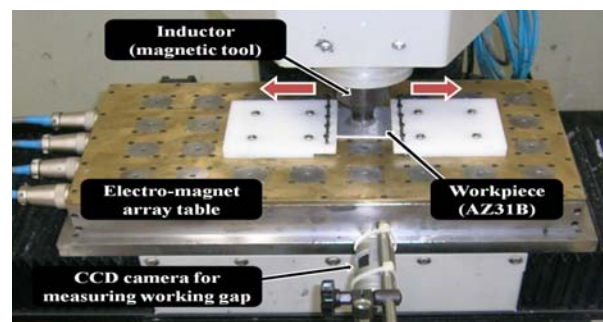


Fig. 9 Experimental setup and procedure for MAP of AZ31B magnesium alloy plate.

TABLE II
FACTORS AND LEVELS USED IN EXPERIMENT

Factors	Levels		
	1	2	3
Current of table, A(A)	0.2	0.5	0.8
Current of tool, B(A)	1.5	2.0	2.5
Spindle speed, C(rpm)	900	1200	1500
Abrasive Weight, D(g)	1.5	2.0	2.5

of magnetic flux density was about 100mT. The spindle speed was used in the range of 900 to 1,500rpm since most abrasive particles could easily fly from working area in high rotational speed over 1,600rpm. The weight of abrasive is represented as total amount of magnetic abrasives including iron powder, abrasive and silicone gel medium. At this experimental, a Taguchi's L₂₇(3⁴) orthogonal array that includes the four factors and three levels was applied. Two-factor interaction was concerned with effectiveness factor on the second generation MAP of AZ31B.

B. Evaluation of Process Parameters and Optimal Condition

Experiments were conducted and then the measured results were evaluated with the help of the signal-to-noise ratio and the ANOVA. Experimental results indicate the improvement of the surface roughness after the MAP. Generally, the signal-to-noise ratio is used to quantify the present variation in the Taguchi method. In this study, the-larger-is-the-better type of the signal-to-noise ratio was selected as the quality characteristic, since the more change in the surface roughness means the better efficiency of the MAP. The S/N ratio (η) is calculated as follows.

$$\eta = -10 \log \left(\frac{1}{n} \sum \frac{1}{y_i^2} \right) \tag{1}$$

Where n represents the number of measurements and y_i is the measured values.

TABLE III
EXPERIMENTAL RESULTS AND CALCULATED S/N RATIO

No.	Enhanced surface roughness(μm)	S/N ratio	No.	Enhanced surface roughness(μm)	S/N ratio
1	0.15	-16.4782	15	0.1	-20
2	0.176	-15.0897	16	0.157	-16.082
3	0.089	-21.0122	17	0.26	-11.7005
4	0.203	-13.8501	18	0.187	-14.5632
5	0.26	-11.7005	19	0.259	-11.734
6	0.09	-20.9151	20	0.254	-11.9033
7	0.197	-14.1107	21	0.26	-11.7005
8	0.147	-16.6537	22	0.229	-12.8033
9	0.127	-17.9239	23	0.213	-13.4324
10	0.124	-18.1316	24	0.196	-14.1549
11	0.213	-13.4324	25	0.189	-14.4708
12	0.156	-16.1375	26	0.161	-15.8635

13	0.196	-14.1549	27	0.23	-12.7654
14	0.273	-11.2767			

TABLE IV
ANOVA FOR EACH FACTOR

	SS	DOF	V	F ₀	F _{0.01}
A	46.777	2	23.388	14.994	10.9
B	0.6190	2	0.309	0.198	10.9
C	44.734	2	22.367	14.339	10.9
D	1.892	2	0.946	0.606	10.9
AxB	20.931	4	5.232	3.354	9.15
AxC	52.155	4	13.038	8.359	9.15
BxC	31.360	4	7.840	5.026	9.15
Error(e)	9.358	6	1.559		
Total	207.829	26			

Both the measured experimental results and calculated S/N ratios were listed in Table III. To evaluate the effect of process factors on the enhanced surface roughness, ANOVA(analysis of variance) was conducted and results are listed in Table IV.

According to Table IV, the current of table had a dominant effect on the improvement of surface roughness in the case of the second generation MAP for AZ31B magnesium alloy. The current of tool and the weight of abrasive were process factors considered in this study that had the least influence on the enhanced surface roughness.

Thus, based on the experimental results obtained in this study, the magnetic force of electro-magnet table played an important role in producing better surface more than the magnetic force generated in inductor. It means that the pressure force on the surface of non-magnetic material was determined by change of magnetic force on the electro-magnet table instead of magnetic force on the inductor, because more magnetic abrasives were constrained on the surface of AZ31B magnesium alloy.

In the Taguchi method, the highest S/N ratio for the result is desirable. As shown in Fig. 11, the level corresponding to the highest S/N ratio in each factor was chosen as the optimum conditions. The selected optimal conditions were A3B2C2D3 (current of table of 0.8A, current of tool of 2.0A, spindle speed of 1200rpm, weight of abrasive of 2.5g). These optimal conditions can minimize the process variability and produce better the surface roughness.

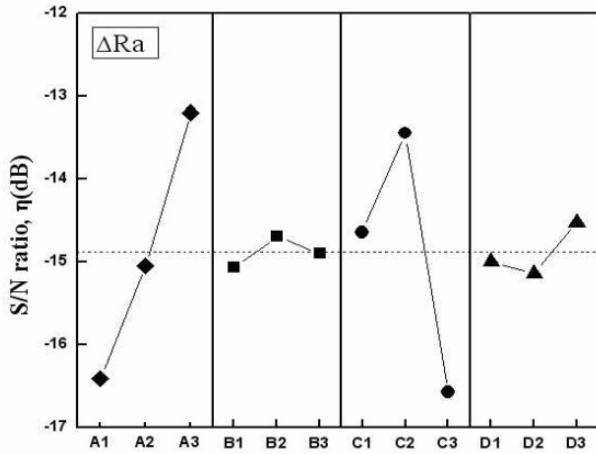


Fig. 10 Influence of polishing factors on surface roughness.

V. DEVELOPMENT OF PREDICTION MODELS

A. Applying Prediction Model Using S/N Ratio

It is desirable to be able to forecast enhanced surface roughness according to the MAP conditions. One means of doing this is to represent predicted enhanced surface roughness mathematically as a function of the applicable MAP parameters and signal-to-noise ratios. So, it is possible to forecast the signal-to-noise ratio of enhanced surface roughness by calculating the function as below.

$$\eta_{sn} = \bar{\eta}_{sn} + (A_i - \bar{\eta}_{sn}) + (B_j - \bar{\eta}_{sn}) + (C_k - \bar{\eta}_{sn}) + (D_l - \bar{\eta}_{sn}) = -3\bar{\eta}_{sn} + (A_i + B_j + C_k + D_l) \quad (2)$$

Where η_{sn} and $\bar{\eta}_{sn}$ represent the signal-to-noise for combination of each MAP parameters and the average value of those. A_i, B_j, C_k and D_l is the signal-to-noise of each parameter according to variation of level. After the statistical analysis, analysis of variance was generated to verify the validation of prediction model using signal-to-noise ratio as shown in Table V. As a result, prediction model was effective to forecast enhanced surface roughness since the statistical Ft values exceeded the critical value of $F_{0.01}=4.33$. Table VI shows the verification of prediction model. It is indicated that the predicted values of enhanced surface roughness well coincide with measured values although it had some wide deviation in optimal condition.

B. Development of Response Surface Model

Second-order response surface models using the current of table A(A), the current of tool B(A), spindle speed C(rpm) and abrasive weight D(g) were developed as below.

$$\Delta Ra = -0.677525238 + 0.046606A + 0.2633557B + 0.00113841C - 0.05471886D + 0.0606419A^2 - 0.056942335B^2 - 0.000000523C^2 + 0.063218003D^2 - 0.029700025AB + 0.000294894AC - 0.145297703AD + 0.0000123BC - 0.023207141BD - 0.0000592CD \quad (3)$$

Where, the symbol ΔR (μm) was the value of enhanced surface roughness. Fig. 11 presents an example of the

TABLE V

	S_i	ϕ_i	V_i	F_{0i}	$F_{0.01}$
Model	0.0427	4	0.0106	4.5597	4.33
Residual	0.0515	22	0.0023		
Total	0.0942	26			

MAP condition	Predicted value	Measured value
$A_3B_2C_2D_3$ (OP)	0.275	0.342
$A_2B_2C_2D_2$	0.207	0.226
$A_3B_3C_3D_3$	0.187	0.209

response surface and contour plots of the enhanced surface roughness according to change of the current of table and the spindle speed. In these plots, the current of tool and weight of abrasive were fixed as 2.0A and 2.5g respectively. The 3D plot seems to rapidly change according to the change of the spindle speed more than current of table. Moreover, from the contour plot shown in Fig. 11 (b), it seen that enhanced surface roughness was increased linearly when the current of table was increased and the spindle speed was fixed. Fig. 12 shows the response surface and contour plots of the enhanced surface roughness according to the change of the current of table and the current of tool. In these plots, it is indicated that the current of table has to be increased to have better surface when the current of tool is fixed. For example, as the current of tool was 2.0A, the current of table should be at least 0.72A to get the enhanced surface roughness of $0.245 \mu m$. The developed second-order response surface model achieved the 99% confidence interval as shown in Table VII then the developed prediction model was verified statistically in this study. Table VIII shows the comparing the confirmatory test results and predicted value.

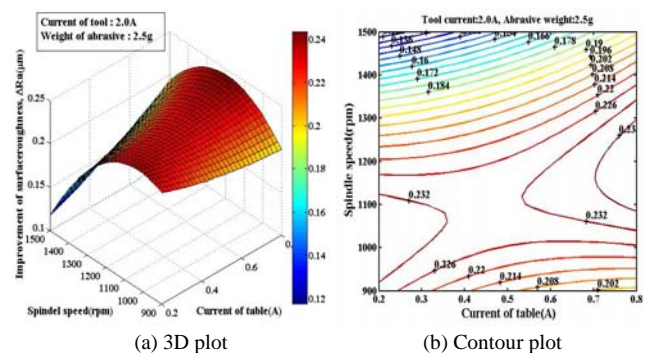


Fig. 11 3D plot and contour plot of second-order RSM for predicting improvement of surface roughness according to the current of table and spindle speed.

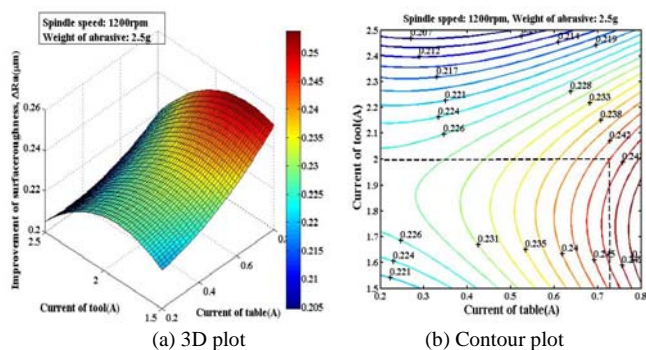


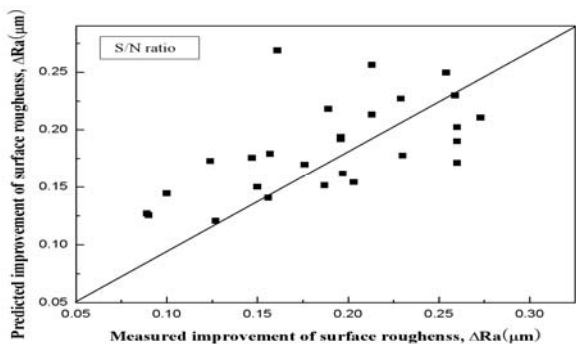
Fig. 12 3D plot and contour plot of second-order RSM for predicting improvement of surface roughness according to the current s of table and tool.

TABLE VII
ANALYSIS OF THE VARIANCE FOR RSM

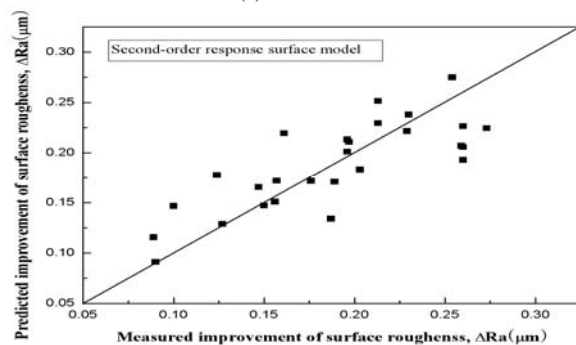
	S_i	ϕ_i	V_i	F_{0i}	$F_{0.01}$
Model	0.0504	14	0.0036	1.5544	0.2248
Residual	0.0278	12	0.0023		
Total	0.0782	26			

TABLE VIII
ANALYSIS OF RESPONSE SURFACE MODEL

MAP condition	Predicted value	Measured value
$A_3B_2C_2D_3(OP)$	0.249	0.342
$A_2B_2C_2D_2$	0.212	0.226
$A_3B_3C_3D_3$	0.173	0.209



(a) S/N ratio



(b) Second-order response surface model

Fig. 13 Correlation between predicted and measured improvement of surface roughness.

Fig. 13 (a) and (b) show the difference between the measured quantities by applying the developed response surface model and prediction model using signal-to-noise

ratio. As shown in Fig. 13 (b), in case of response surface model, the predicted enhanced surface roughness coincides with the measured value more than in case of prediction model using signal-to-noise ratio. Thus, based on the results, the response surface model is suitable for predicting enhanced surface roughness after second generation MAP of AZ31B more than prediction model using signal-to-noise ratio.

VI. CONCLUSION

In this study, second generation MAP process including electro-magnet array table was used for polishing of AZ31B magnesium alloy. The evaluation of the MAP of AZ31B was performed using Taguchi method. Moreover, prediction models using response surface model and signal-to-noise ratio were developed. The obtained conclusions are as follow.

- 1) To improve magnetic force on the surface of magnesium alloy, electro-magnet array table was installed in second generation MAP. As a result of simulation and experimental verification in case of distribution and maximum magnitude of magnetic flux density were larger than in case of arrangement of identical magnet pole.
- 2) The current of table had a dominant effect on the improvement of surface roughness in the case of the second generation MAP for AZ31B magnesium alloy. However, the current of tool and the weight of abrasive were process factors considered in this study that had the least influence on the enhanced surface roughness.
- 3) The optimal conditions for the second generation MAP of AZ31B plate were applied current of table of 0.8A, current of tool of 2.0A, spindle speed of 1200rpm and weight of abrasive of 2.5g.
- 4) The prediction models were developed by response surface model and signal-to-noise ratio. Based on the results, the response surface model is suitable for predicting surface roughness after second generation MAP of AZ31B more than prediction model using signal-to-noise ratio.

ACKNOWLEDGMENT

This study was supported by Basic Science Program through the National Research Foundation of Korea (NRF) funded by the Ministry of Education, Science and Technology (Grant No. 2010-0015271).

REFERENCES

- [1] G. Garcés, F. Domínguez, P. Pérez, G. Caruana and P. Adeva, "Effect of extrusion temperature on the microstructure and plastic deformation of PM-AZ92," *Journal of Alloys and Compounds*, vol. 422, no. 1-2, pp. 293-298, Sep. 2006.
- [2] Z. M. Zhang, H. Y. Xu and Q. Wang, "Corrosion and mechanical properties of hot-extruded AZ31 magnesium alloys," *Transactions of Nonferrous Metals Society of China*, vol. 18, no. 1, pp. 140-144, Dec. 2008.
- [3] B. Jing, S. Yangshan, X. Shan, X. Feng and Z. Tianbai, "Microstructure and tensile creep behavior of Mg-4Al based magnesium alloys with alkaline-earth elements Sr and Ca additions," *Materials Science and Engineering : A*, vol. 419, no. 1-2, pp. 181-188, Mar. 2006.

- [4] H. Michael, L. Martin, B. Katrin and R. Walter, "Fatigue properties of the hot extruded magnesium alloy AZ31," *Materials Science and Engineering : A*, vol. 527, no. 21-22, pp. 5514-5521, Aug. 2010.
- [5] S. O. Kim and J. S. Kwak, "Magnetic force improvement and parameter optimization for magnetic abrasive polishing of AZ31 magnesium alloy," *Transactions of Nonferrous Metals Society of China*, vol. 18, no. 1, pp. 369-373, Dec. 2008.
- [6] S. Yin and T. Shinmura, "A comparative study : polishing characteristics and its mechanisms of three vibration modes in vibration-assisted magnetic abrasive polishing," *International Journal of Machine Tools and Manufacture*, vol. 44, no. 4, pp. 383-390, Mar. 2004.
- [7] S. Yin and T. Shinmura, "Vertical vibration-assisted magnetic abrasive finishing and deburring for magnesium alloy," *International Journal of Machine Tools and Manufacture*, vol. 44, no. 12-13, pp. 1297-1303, Oct. 2004.
- [8] J. S. Kwak, "Enhanced magnetic abrasive polishing of non-ferrous metals utilizing a permanent magnet," *International Journal of Machine Tools and Manufacture*, vol. 49, no. 7-8, pp. 613-618, Jun. 2009.
- [9] A. C. Wang and S. J. Lee, "Study the characteristics of magnetic finishing with gel abrasive," *International Journal of Machine Tools and Manufacture*, vol. 49, no. 14, pp. 1063-1069, Nov. 2009.